



Single-Axis Tracker Control Optimization Potential for the Contiguous United States

Preprint

Kevin Anderson¹ and Saurabh Aneja²

1 National Renewable Energy Laboratory

2 FTC Solar

Presented at the 49th IEEE Photovoltaic Specialists Conference (PVSC 49)

Philadelphia, Pennsylvania

June 5-10, 2022

**NREL is a national laboratory of the U.S. Department of Energy
Office of Energy Efficiency & Renewable Energy
Operated by the Alliance for Sustainable Energy, LLC**

This report is available at no cost from the National Renewable Energy Laboratory (NREL) at www.nrel.gov/publications.

Contract No. DE-AC36-08GO28308

Conference Paper
NREL/CP-5K00-82811
July 2022



Single-Axis Tracker Control Optimization Potential for the Contiguous United States

Preprint

Kevin Anderson¹ and Saurabh Aneja²

1 National Renewable Energy Laboratory

2 FTC Solar

Suggested Citation

Anderson, Kevin and Saurabh Aneja. 2022. *Single-Axis Tracker Control Optimization Potential for the Contiguous United States: Preprint*. Golden, CO: National Renewable Energy Laboratory. NREL/CP-5K00-82811 <https://www.nrel.gov/docs/fy22osti/82811.pdf>.

© 2022 IEEE. Personal use of this material is permitted. Permission from IEEE must be obtained for all other uses, in any current or future media, including reprinting/republishing this material for advertising or promotional purposes, creating new collective works, for resale or redistribution to servers or lists, or reuse of any copyrighted component of this work in other works.

**NREL is a national laboratory of the U.S. Department of Energy
Office of Energy Efficiency & Renewable Energy
Operated by the Alliance for Sustainable Energy, LLC**

This report is available at no cost from the National Renewable Energy Laboratory (NREL) at www.nrel.gov/publications.

Contract No. DE-AC36-08GO28308

Conference Paper
NREL/CP-5K00-82811
July 2022

National Renewable Energy Laboratory
15013 Denver West Parkway
Golden, CO 80401
303-275-3000 • www.nrel.gov

NOTICE

This work was authored in part by the National Renewable Energy Laboratory, operated by Alliance for Sustainable Energy, LLC, for the U.S. Department of Energy (DOE) under Contract No. DE-AC36-08GO28308. Funding provided by the U.S. Department of Energy Office of Energy Efficiency and Renewable Energy under Solar Energy Technologies Office (SETO) Agreement Numbers 34348. The views expressed herein do not necessarily represent the views of the DOE or the U.S. Government. The U.S. Government retains and the publisher, by accepting the article for publication, acknowledges that the U.S. Government retains a nonexclusive, paid-up, irrevocable, worldwide license to publish or reproduce the published form of this work, or allow others to do so, for U.S. Government purposes.

This report is available at no cost from the National Renewable Energy Laboratory (NREL) at www.nrel.gov/publications.

U.S. Department of Energy (DOE) reports produced after 1991 and a growing number of pre-1991 documents are available free via www.OSTI.gov.

Cover Photos by Dennis Schroeder: (clockwise, left to right) NREL 51934, NREL 45897, NREL 42160, NREL 45891, NREL 48097, NREL 46526.

NREL prints on paper that contains recycled content.

Single-Axis Tracker Control Optimization Potential for the Contiguous United States

Kevin Anderson¹ and Saurabh Aneja²

¹National Renewable Energy Laboratory, Golden, CO, 80401, USA

²FTC Solar, Austin, TX, 78759, USA

Abstract—Conventional tracker control algorithms maximize collection of direct irradiance with no regard for collection of diffuse irradiance. Therefore, a tracker control algorithm that optimizes for maximal total irradiance, not just direct, might realize improved insolation collection. Using weather data gridded at 0.25° by 0.25° latitude/longitude spacing covering the contiguous United States, we evaluate the insolation gain of two alternative control algorithms optimized for improved total irradiance collection in monofacial arrays and present annual and monthly geographic heatmaps showing the gains across the contiguous United States. Certain locations show potential annual insolation gains approaching 1.0%, but most locations with recently-built tracker systems show annual gains between 0.1% and 0.4%. We also demonstrate a relationship between a climate’s annualized diffuse insolation fraction and its potential tracker optimization insolation gain.

Index Terms—photovoltaic, single-axis, tracking, optimization, insolation, diffuse

I. INTRODUCTION

Minimizing the angle of incidence is the foundation of conventional single-axis tracking strategies. The angle of incidence (AOI), a measure of the degree of alignment between a collector and the sun, is the angle between the collector orientation and solar position vectors. The collector’s exposure to direct irradiance from the sun is maximized when AOI is zero, prompting the use of AOI minimization as the basis of tracking. Furthermore, closed-form expressions based on solar position and tracker geometry are available for calculating the tracker rotation that minimizes AOI [1]–[3], making an AOI-based strategy straightforward to implement in practice. Trackers that follow the AOI-minimized rotation are said to “true-track” (often with “backtracking” adjustments to prevent self-shading) and have until recently been the main focus of the single-axis tracker market. This strategy is also called the “astronomical” strategy for its focus on the solar disc’s position in the sky.

However, optimizing for direct irradiance alone is suspect in the context of non-concentrating photovoltaic (PV) systems. In contrast to concentrating collectors, typical flat-plate photovoltaic arrays harvest both direct and diffuse irradiance, motivating a tracking strategy that maximizes total in-plane irradiance, not just the direct component. This is made most evident by considering overcast sky conditions when diffuse irradiance dominates: there is nothing to gain by prioritizing alignment with solar position in the absence of direct irradiance, so attention should instead be turned

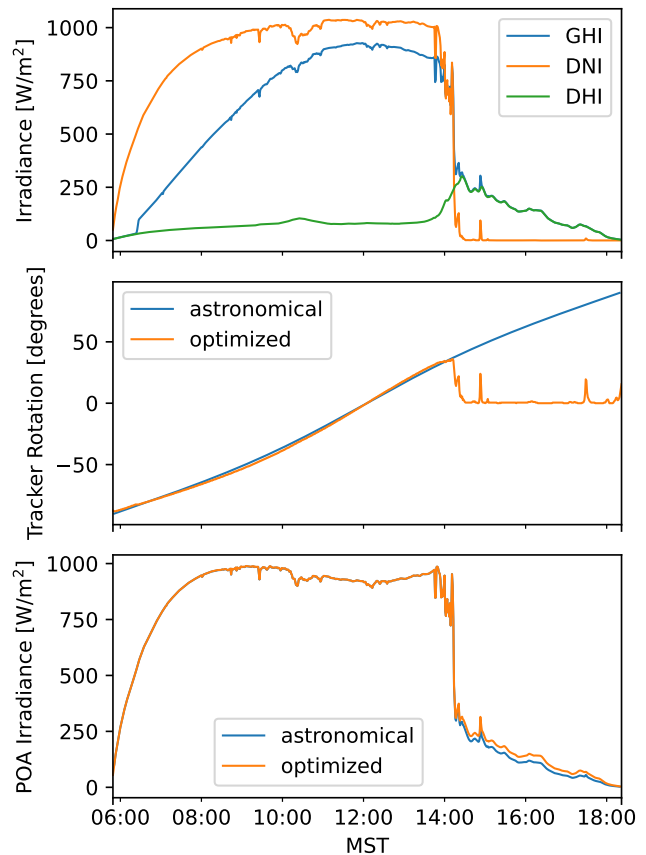


Fig. 1. Example comparison of rotation and simulated irradiance curves for the conventional astronomical tracking strategy and a tracking strategy optimized for total irradiance capture. This alternative strategy can outperform the conventional astronomical strategy, especially in diffuse conditions.

towards the diffuse components originating from the sky dome and reflected from the ground. Even under clear skies these diffuse components still contribute to total incident irradiance, meaning the irradiance-maximized rotation may differ from the true-tracking rotation under all sky conditions.

Fig. 1 compares the simulated in-plane irradiances corresponding to a tracker using the astronomical strategy with one maximizing global incident irradiance. Under the clear skies in the morning, the optimized strategy only very slightly outperforms the astronomical strategy. In this case the difference is so small it is not visible in the figure. However, the astronomical

strategy is noticeably outperformed by the optimized strategy under cloudy skies in the later part of the day. The irradiance data in this example came from the Baseline Measurement System at the National Renewable Energy Laboratory’s Solar Radiation Research Laboratory [4].

The general concept of considering diffuse irradiance in dual- and single-axis tracker control has been previously investigated for select ground station locations [5]–[9], often corresponding to locations in the Baseline Surface Radiation Network (BSRN) [10], a global network of high-quality irradiance measurement stations. It is worth emphasizing that multiple styles of diffuse-aware tracking have been considered in the literature; most existing studies used horizontal orientation as the alternative to conventional tracking, but some studies [8] instead opted to use the tracker rotation that maximizes incident irradiance according to a particular irradiance transposition model. Some studies have also considered this optimization in the context of bifacial PV arrays [11], [12]; in this work we focus exclusively on front-side irradiance.

In this work we evaluate the potential insolation gain of two single-axis tracker optimization strategies. In contrast to previous studies based on ground station data, the insolation gain is evaluated using gridded weather data, allowing detailed geographic gain comparison across the contiguous United States. Finally, the potential gain is evaluated at locations of existing utility-scale tracking systems.

II. METHODS

The approach is relatively straightforward: for every gridded location in our area of interest, apply each tracker strategy to a weather dataset for that location and model the total annual insulations. The details of each step are as follows:

A. Tracking Strategies

We consider three tracking strategies:

- 1) *Astronomical*: the conventional AOI-minimized rotation as implemented by common tracker controllers today.
- 2) *All-times*: the rotation that maximizes incident irradiance, identified via brute force search, considering all times of day.
- 3) *Between-backtracking*: similar to the “all-times” strategy, except only non-backtracking times (i.e., the portion of the day between the morning and evening backtracking periods) are considered.

The motivation for the between-backtracking strategy may deserve explanation. In certain conditions or situations, perceived or practical limitations may prevent system operators from extending the irradiance optimization methods presented here from being used during backtracking hours. For example, operators may determine that irradiance forecast data needed for rotation determination has less certainty than backtracking processes already employed at existing systems. For this reason, we also calculated insolation gains from times periods outside of backtracking hours only.

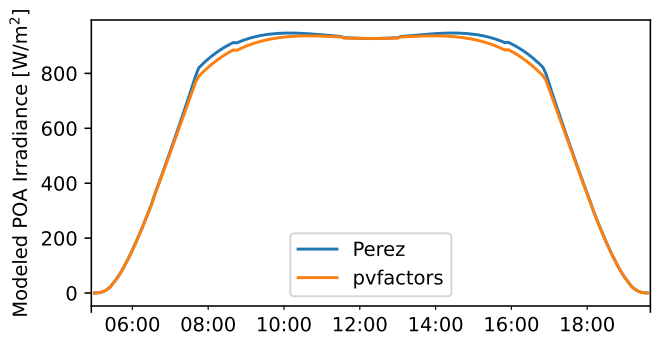


Fig. 2. Example comparison of simulated plane of array (POA) irradiance using the base Perez transposition model and unshaded ground and the same accounting for sky diffuse shading and ground shading using pvfactors.

TABLE I
PVFACTORS MODELING ASSUMPTIONS

Parameter	Value
Row Count	5
Axis Alignment	North-South
Axis Tilt [degrees]	0
Axis Height [m]	3.0
Collector Width [m]	4.0
Ground Coverage Ratio	0.3
Ground Albedo	0.2

Insolation gains for the “all-times” and “between-backtracking” strategies are calculated relative to the astronomical method. In each case the rotation angle is constrained [1], [3] so that rows do not subject each other to direct shading, assuming uniform flat terrain.

B. Incident Irradiance Model

Detailed investigation of tracker rotation optimization warrants a detailed incident irradiance model. In this work we use pvfactors, a detailed transposition and view factor model [13], [14]. By including the effect of row-to-row sky diffuse shading, ground shadows, and module-module reflections as pvfactors does, the modeled irradiance should be more representative of the irradiance incident on an interior row in a PV array, which will generally be somewhat less than the irradiance measured by an isolated radiometer. Fig. 2 shows an example of this difference, comparing the output of the pvfactors model with the output of the Perez irradiance transposition model [15] on which it is based.

In this work we simulated irradiance for the center row of an array with the specifications listed in Table I.

C. Weather Data

Annual weather files for a 0.25° by 0.25° grid covering the contiguous United States were retrieved from the Physical Solar Model v3 (PSM3), part of the National Solar Radiation Data Base (NSRDB) [16]. For this work we select hourly Typical Meteorological Year (TMY) data from the latest “tmy-2020” dataset. TMYs exclude unusual weather conditions, meaning a TMY-based analysis is less likely to be influenced



Fig. 3. Locations of utility-scale single-axis tracking PV systems in the 2021 LBNL utility-scale solar database. Color indicates system DC capacity in MW on a logarithmic scale.

by prolonged atypical cloudy or clear periods. In total, this dataset covers over 13000 locations and requires roughly 11 GB to store in uncompressed CSV form.

D. Tracking System Locations

The economic arguments for preferring some regions over others when deploying tracking systems are well established. Thus, it is of interest to examine the modeled insolation gains considering only the subset of locations deemed suitable for tracking systems. We identify suitable locations using the locations of existing tracking systems as a proxy. The locations of existing single-axis tracking PV systems were retrieved from a database of utility-scale systems assembled by Lawrence Berkeley National Laboratory (LBNL) [17]. The 2021 edition of this database includes 660 utility-scale single-axis tracking systems ranging in size from 5 to 500 MWdc. Fig. 3 shows the locations and DC capacities of these systems.

The spatial distribution of these tracking systems is also evolving over time. For example, the database’s commercial operation date (COD) records go back to 2007 but the oldest of the 35 systems in Oregon reached COD only in 2016. It seems reasonable to expect this trend of tracking systems expanding into more diffuse climates to continue in the future. Because the spatial distribution of tracking system locations is evolving over time, so too is the distribution of insolation gains at those locations. For this reason we examine not only the modeled insolation gains for all tracker system locations but also the insolation gains partitioned by system COD year.

III. RESULTS

Figs. 4 and 5 show the annualized and monthly potential insolation gain for the all-times strategy. The insolation gains for the between-backtracking times are very similar to those of the all-times strategy (see Fig. 6) and therefore not shown here.

Fig. 7 shows the distribution of insolation gains partitioned by hour of day. The largest gains are concentrated around mid-morning and mid-afternoon, consistent with the intuition that the largest gains come from times of day when the astronomical algorithm results in steep tracker rotations and

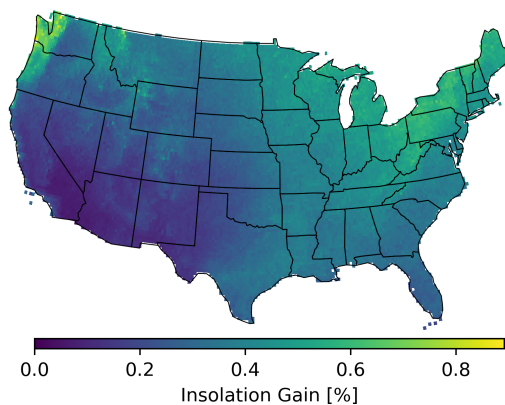


Fig. 4. Annual insolation gain for the all-times strategy. Color shows the increase (in percent) in annual insolation relative to the astronomical tracking strategy.

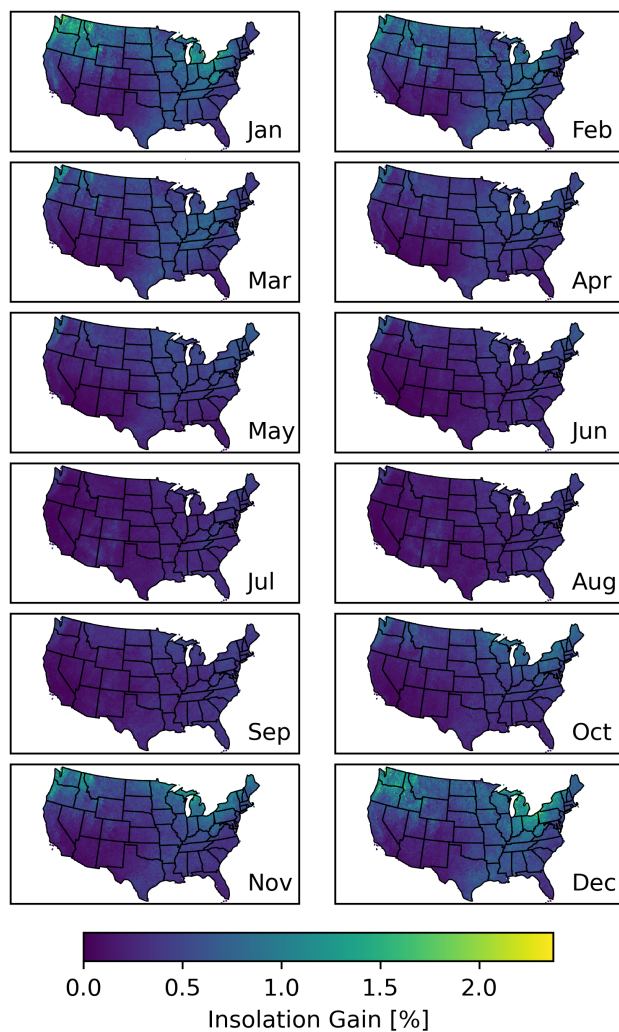


Fig. 5. Monthly insolation gains for the all-times strategy. Color shows the increase in insolation relative to the astronomical tracking strategy, with the largest relative gains being achieved in winter.

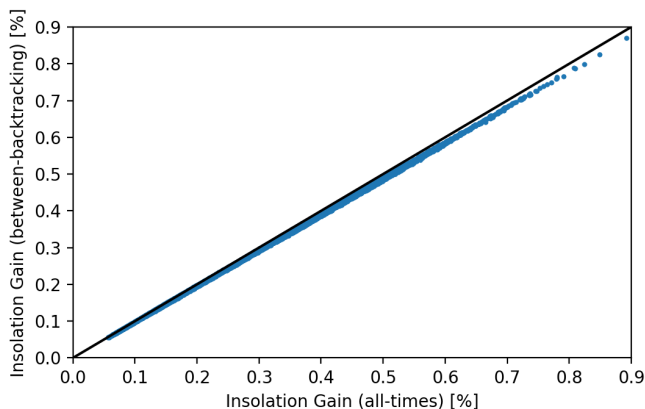


Fig. 6. Annual insolation gain comparison for the all-times and between-backtracking strategies, showing only a marginal decrease (less than 3% relative/.01% absolute) in annual insolation gain by excluding backtracking times. The black line indicates a perfect $y = x$ relationship for reference.

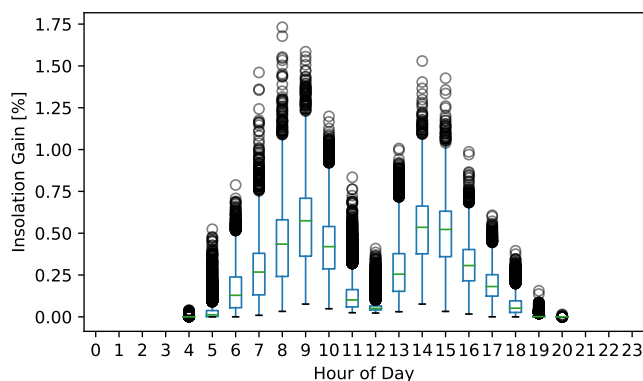


Fig. 7. Distribution of annual insolation gains for all locations, partitioned by hour of day, for the all-times strategy. For example, the hour=9 distribution reflects the annual insolation gain considering only the 365 hour long intervals from 9–10 AM (local standard time) in each year. Each value in the distribution represents the annual partitioned gain for a single location. Gains are concentrated around times of day where the astronomical strategy would orient modules at steep tilts.

is therefore most different from a diffuse-optimized horizontal rotation.

Fig. 8 shows the distribution of potential gains for the all-times strategy at locations of tracking systems in the LBNL utility-scale dataset, partitioned by COD year.

Finally, Fig. 9 shows how, for each location in the 0.25° by 0.25° grid, the potential all-times insolation gain varies with that location's diffuse insolation fraction. The diffuse insolation fraction is the fraction of annual global horizontal insolation (GHI) contributed by diffuse horizontal insolation (DHI). The cloudier the climate, the generally higher the diffuse fraction will be.

IV. DISCUSSION

Consistent with previous studies [7], Fig. 4 shows that insolation gains are strongly dependent on climate; potential

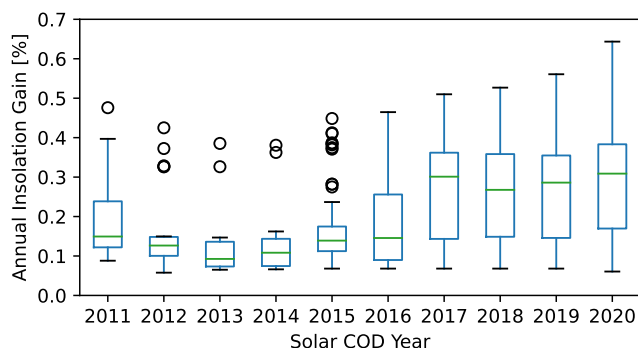


Fig. 8. Distribution of annual insolation gains using the all-times optimization for locations of tracking systems in the LBNL database, partitioned by system commercial operation year. The annual gains show a general upwards trend with time. Years before 2011 are not shown due to their small number of systems.

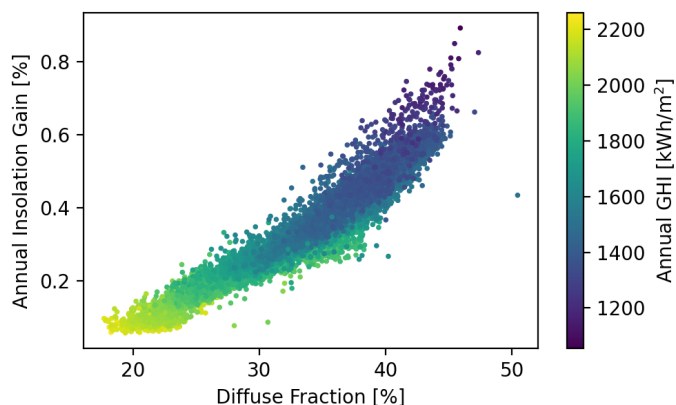


Fig. 9. Relationship between annual all-times insolation gain and annual diffuse fraction, colored by total annual global horizontal insolation (GHI). Locations with more diffuse skies (larger diffuse fraction) tend to have larger potential tracker optimization gain.

gain in the desert Southwest is negligible, but other parts of the country see potential gains from 0.5% to a peak of over 0.8% in the Pacific Northwest for the all-times strategy. The potential gains for the between-backtracking strategy show nearly identical spatial trends and are only marginally reduced compared to the all-times strategy, suggesting that the large majority of potential insolation gains occur outside of backtracking times. This finding is further confirmed in Fig. 7.

The monthly heatmaps in Fig. 5 show that the largest relative insolation gains occur in the North American winter, reaching monthly values approaching 2.5% in some locations. However, it is worth pointing out that large relative winter gains may be smaller in an absolute sense than small relative summer gains due to overall seasonality in solar resource.

Although Fig. 8 does show a trend of increasing potential insolation gain over time, the trend has stagnated since 2017. Together with Fig. 9, showing that diffuse climates tend to have larger potential gains, this suggests that new projects have

not been pushing into more diffuse climates since 2017. This finding is consistent with the conclusions of the LBNL report itself [17], which reports stable global horizontal insolation at all utility-scale solar sites (not just tracking PV) since 2017.

Now we discuss several caveats in these results. The ground-reflected component of incident irradiance depends strongly on ground albedo. Ground albedo varies not only with substrate type but also with weather conditions, primarily snowfall. In this work we have assumed a static albedo of 0.2 for all conditions. A more detailed analysis would consider not only geographic variation in ground albedo (e.g. bare soil versus grass) but also the effect of snowfall. A secondary consideration is that this optimization neglects the varying spectral mismatch of each irradiance component with the spectral response of PV absorbers.

An additional concern is that hourly TMYs may lack the resolution needed to fully capture the potential for irradiance-based tracker optimization. A full discussion of the limitations of satellite-based irradiance is out of scope here, but this is a problem both spatially (due to the kilometer-scale size of each satellite pixel) as well as temporally (hourly data cannot resolve subhourly variability, which can be significant in some climates). Future work may include comparing the gains modeled using TMYs with the gains modeled using higher resolution satellite data or ground station measurements.

V. CONCLUSIONS

Based on hourly TMY data, we find that the potential insolation gain over the conventional astronomical tracking algorithm depends strongly on local climate, especially the fraction of diffuse annual insolation, with potential annual gains ranging from near-zero in the desert Southwest to over 0.8% in the Pacific Northwest. Typical gains for locations with recently-installed tracking systems range from 0.2–0.4%. The gains also show significant seasonality, with monthly gains as high as 2.4% in winter for some locations. Finally, these results show that omitting backtracking times of day from the irradiance optimization reduces the potential gain only slightly.

ACKNOWLEDGMENT

The authors wish to thank the maintainers of the NSRDB and the LBNL utility-scale solar database. The authors additionally thank the developers of the open-source software packages used in this work (pvfactors, pvlib, and the broader scientific python ecosystem) and highlight the value that open-source software brings to the research community.

This work was authored in part by Alliance for Sustainable Energy, LLC, the manager and operator of the National Renewable Energy Laboratory for the U.S. Department of Energy (DOE) under Contract No. DE-AC36-08GO28308. Funding provided by the U.S. Department of Energy’s Office of Energy Efficiency and Renewable Energy (EERE) under Solar Energy Technologies Office (SETO) Agreement Numbers 34348. The views expressed in the article do not necessarily represent the views of the DOE or the U.S. Government. The U.S.

Government retains and the publisher, by accepting the article for publication, acknowledges that the U.S. Government retains a nonexclusive, paid-up, irrevocable, worldwide license to publish or reproduce the published form of this work, or allow others to do so, for U.S. Government purposes.

REFERENCES

- [1] E. Lorenzo, L. Narvarte, and J. Muñoz, “Tracking and backtracking,” *Progress in Photovoltaics: Research and Applications*, vol. 19, no. 6, pp. 747–753, Feb. 2011. [Online]. Available: <https://doi.org/10.1002/PIP.1085>
- [2] W. F. Marion and A. P. Dobos, “Rotation angle for the optimum tracking of one-axis trackers,” National Renewable Energy Laboratory, Tech. Rep. NREL/TP-6A20-58891, 2013. [Online]. Available: <https://doi.org/10.2172/1089596>
- [3] K. Anderson and M. Mikofski, “Slope-aware backtracking for single-axis trackers,” National Renewable Energy Laboratory, Tech. Rep. NREL/TP-5K00-76626, Jul. 2020. [Online]. Available: <https://doi.org/10.2172/1660126>
- [4] A. Andreas and T. Stoffel, “NREL Solar Radiation Research Laboratory (SRRL): Baseline Measurement System (BMS),” National Renewable Energy Laboratory, Tech. Rep. DA-5500-56488, 1981. [Online]. Available: <http://dx.doi.org/10.5439/1052221>
- [5] N. A. Kelly and T. L. Gibson, “Improved photovoltaic energy output for cloudy conditions with a solar tracking system,” *Solar Energy*, vol. 83, no. 11, pp. 2092–2102, Nov. 2009. [Online]. Available: <https://doi.org/10.1016/j.solener.2009.08.009>
- [6] —, “Increasing the solar photovoltaic energy capture on sunny and cloudy days,” *Solar Energy*, vol. 85, no. 1, pp. 111–125, Jan. 2011. [Online]. Available: <https://doi.org/10.1016/j.solener.2010.10.015>
- [7] J. Antonanzas, R. Urraca, F. M. de Pison, and F. Antonanzas, “Optimal solar tracking strategy to increase irradiance in the plane of array under cloudy conditions: A study across Europe,” *Solar Energy*, vol. 163, pp. 122 – 130, 2018. [Online]. Available: <https://doi.org/10.1016/j.solener.2018.01.080>
- [8] C. D. Rodriguez-Gallegos, O. Gandhi, S. K. Panda, and T. Reindl, “On the PV tracker performance: Tracking the sun versus tracking the best orientation,” *IEEE Journal of Photovoltaics*, vol. 10, no. 5, pp. 1474–1480, Sep. 2020. [Online]. Available: <https://doi.org/10.1109/jphotov.2020.3006994>
- [9] G. Quesada, L. Guillon, D. R. Rousse, M. Mehtash, Y. Dutil, and P.-L. Paradis, “Tracking strategy for photovoltaic solar systems in high latitudes,” *Energy Conversion and Management*, vol. 103, pp. 147–156, Oct. 2015. [Online]. Available: <https://doi.org/10.1016/j.enconman.2015.06.041>
- [10] A. Driemel *et al.*, “Baseline surface radiation network (BSRN): structure and data description (1992–2017),” *Earth Syst. Sci. Data*, no. 10, pp. 1491–1501, 2018. [Online]. Available: <https://doi.org/10.5194/essd-10-1491-2018>
- [11] S. A. Pelaez, C. Deline, P. Greenberg, J. S. Stein, and R. K. Kostuk, “Model and validation of single-axis tracking with bifacial PV,” *IEEE Journal of Photovoltaics*, vol. 9, no. 3, pp. 715–721, May 2019. [Online]. Available: <https://doi.org/10.1109/jphotov.2019.2892872>
- [12] K. R. McIntosh, M. D. Abbott, and B. A. Sudbury, “The optimal tilt angle of monofacial and bifacial modules on single-axis trackers,” *IEEE Journal of Photovoltaics*, vol. 12, no. 1, pp. 397–405, Jan. 2022. [Online]. Available: <https://doi.org/10.1109/jphotov.2021.3126115>
- [13] M. A. Anoma, D. Jacob, B. C. Bourne, J. A. Scholl, D. M. Riley, and C. W. Hansen, “View factor model and validation for bifacial PV and diffuse shade on single-axis trackers,” in *2017 IEEE 44th Photovoltaic Specialist Conference (PVSC)*. IEEE, Jun. 2017. [Online]. Available: <https://doi.org/10.1109/pvsc.2017.8366704>
- [14] “pvfactors v1.5.2 (GitHub Repository),” 2021. [Online]. Available: <https://github.com/sunpower/pvfactors>
- [15] R. Perez, P. Ineichen, R. Seals, J. Michalsky, and R. Stewart, “Modeling daylight availability and irradiance components from direct and global irradiance,” *Solar Energy*, vol. 44, no. 5, pp. 271–289, 1990. [Online]. Available: [https://doi.org/10.1016/0038-092X\(90\)90055-H](https://doi.org/10.1016/0038-092X(90)90055-H)
- [16] M. Sengupta, Y. Xie, A. Lopez, A. Habte, G. Maclaurin, and J. Shelby, “The national solar radiation data base (NSRDB),” *Renewable and Sustainable Energy Reviews*, vol. 89, pp. 51–60, 2018. [Online]. Available: <https://doi.org/10.1016/j.rser.2018.03.003>

- [17] M. Bolinger, J. Seel, C. Warner, and D. Robson, "Utility-scale solar, 2021 edition: Empirical trends in deployment, technology, cost, performance, PPA pricing, and value in the United States," Lawrence Berkely National Laboratory, Tech. Rep., 10 2021. [Online]. Available: <https://www.osti.gov/biblio/1823604>